

Onset of polymer entanglement

Shirish M. Chitanvis

*Theoretical Division, Los Alamos National Laboratory
Los Alamos, New Mexico 87545*

(February 1, 2008)

We have developed a theory of polymer entanglement using an extended Cahn-Hilliard functional, with two extra terms. One is a nonlocal attractive term, operating over mesoscales, which is interpreted as giving rise to entanglement, and the other a local repulsive term indicative of excluded volume interactions. This functional can be derived using notions from gauge theory. We go beyond the Gaussian approximation, to the one-loop level, to show that the system exhibits a crossover to a state of entanglement as the average chain length between points of entanglement decreases. This crossover is marked by *critical* slowing down, as the effective diffusion constant goes to zero. We have also computed the tensile modulus of the system, and we find a corresponding crossover to a regime of high modulus. The single parameter in our theory is obtained by fitting to available experimental data on polystyrene melts of various chain lengths. Extrapolation of this fit yields a model for the cross-over to entanglement. The need for additional experiments detailing the cross-over to the entangled state is pointed out.

PACS: 61.41.+e, 83.10.Nn

I. INTRODUCTION

While it has long been known that entanglement in homopolymers has an important effect on its strength, a thoroughly satisfactory theory of polymer entanglement is still a topic of current research. The classic experimental work of Moore and Watson¹ showed that the bulk modulus of cross-linked natural rubbers depends inversely on the average chain length (N_c) between cross-links in the system, and that end corrections become negligible as the total average molecular weight μ gets very large. They pointed out the analogy between chemical cross-linking and physical entanglement. Thus their work applies in a qualitative sense to entangled systems as well. Their work extended the earlier pioneering work of Flory et al^{2,3}.

Edwards developed the tube theory of the effect of entanglement on elastic moduli of homopolymers using deGennes's idea of reptation³. This theory showed how entanglement enhances the tensile modulus of a homopolymer. He also developed a more detailed model of entangled ring polymers using notions from knot theory⁴. The basic idea behind this theory is an analogy between certain mathematical invariants describing intertwined loops and magnetic fields induced in wires by current-carrying loops. Prager and Frisch⁵ worked on this notion as well, as did Koniaris and Muthukumar⁶.

More recently, interest has turned towards computer simulations of polymer networks, involving various levels of molecular detail, to understand the effect of entanglement on the strength of homopolymers. As examples, we mention the work of Termonia⁷ and Bicerano⁸, who use phenomenological models of polymer networks to study their viscoelastic properties. Comparison with experimental data shows a varying degree of success, depending on the particular system studied. Holtzl et al⁹ use the

more basic fluctuating bond theory to model a network of polyethylene strands to show that entanglement leads to non-affine displacements under large tensile strains.

In an earlier paper,¹⁰ we developed a gauge theory of self-assembly, and utilized renormalization group ideas to study the onset of self-assembly in diblock copolymers. In this paper, we shall pursue a similar continuum approach to understand entanglement.

Intuitively, one can see that entanglement could be described by assuming two extra terms in the Cahn-Hilliard functional,¹¹ one of which is a nonlocal attractive term, which gives rise to entanglement and the other, a soft-core local repulsive term which arises from the fact that the strands cannot cut across each other. We connect the parameters which appear in our theory to the underlying chain parameters with a simple model. We have shown (see Appendix A) how such a functional can be derived naturally using notions from gauge theory.

The results derived from our continuum formulation will be seen to be reminiscent of the chain-theory approaches of Kavassalis and Noolandi¹² for flexible polymer networks, and that of Kroy and Frey¹³ for semi-flexible networks. They utilized a mean-field approach to locate the transition to the state of entanglement. Our theory is also somewhat similar to the paper of Castillo and Geldart¹⁴, who use a ϕ^3 field theory, coupled to the replica trick (in the mean field approximation) of Deam and Edwards¹⁵ to study the vulcanization transition.

We shall utilize a field theoretic approach and go beyond the Gaussian approximation in this paper to show that the onset of the state of entanglement is a crossover phenomenon, rather than a pure phase transition, in that the effective diffusion constant goes to zero at the transition point, but the correlation length and the structure factor do not diverge. A physical reason that fluctuations become important near the onset of the state of entan-

lement is that the average chain length between points of entanglement gets smaller, while in a vulcanized polymer, the cross-links make the system increasingly stiff. This underscores a difference between vulcanization and entanglement- An entangled network of polymers is more dynamic than a vulcanized network. The mean field approximation is expected to be correct¹⁶ for the vulcanization transition.

We have also computed the tensile modulus of the system. Corresponding to the critical slowing down discussed above, we find a crossover in the modulus to a regime of high values. Fits to available experimental data shows how the single parameter in our theory can be parameterized in terms of the molecular weight of the system. Extrapolation of the parameterization we have provided in this paper displays the cross-over to the entangled state. The need for further experiments detailing this cross-over is pointed out.

II. A FIELD THEORY OF ENTANGLEMENT

The continuum, mesoscale approach adopted in this paper assumes that we have performed some spatial averaging of our polymeric system, so that the *order parameter* is the local concentration of the polymers. Our mesoscopic theory of entanglement in polymers is based on the intuitive notion that physical entanglement can be captured by a non-local attraction between the polymers which causes them to remain in proximity. There must be a balancing, repulsive local energy term which says that the polymers cannot cut across each other. The starting point of our mesoscale theory is an internal energy functional which is quadratic in the gradient of the local number concentration. For the moment, we will consider isolated systems, so that the quantity that is conserved is the internal energy¹⁷. We will shortly consider entropy effects as well. Consider the following form for the energy functional:

$$\beta U_0 = \beta \int u_0(c(\mathbf{s})) d^3 s \quad (1)$$

$$\beta = \frac{1}{kT} \quad (2)$$

$$\beta u_0(c(\mathbf{s})) = \left(\frac{g}{2}\right) \frac{\partial c(\mathbf{s})}{\partial s_i} \frac{\partial c(\mathbf{s})}{\partial s_i} \quad (3)$$

where repeated indices are summed over, \mathbf{s} is a dimensionless co-ordinate variable, k is Boltzmann's constant, T is the temperature, and c is the number concentration of the specie. The local concentration c is normalized by dividing by some characteristic inverse volume. The constant g is analogous to a dimensionless diffusion constant. Such energy functionals have been considered over many years as contributing to the total internal energy of

both unary and binary mixtures.¹¹ We will use this form as our starting point to suggest a more complete energy functional:

$$\beta U_{\text{eff}} = \beta U_0 + \left(\frac{\alpha^2}{2}\right) \int d^3 s c(\mathbf{s}) c(\mathbf{s}) - \left(\frac{\gamma}{2\pi}\right) \int d^3 s \int d^3 s' c(\mathbf{s}) \frac{\exp(-\delta|\mathbf{s} - \mathbf{s}'|)}{|\mathbf{s} - \mathbf{s}'|} c(\mathbf{s}') \quad (4)$$

where α^2, γ, δ are positive constants. The local repulsive term is indicative of the fact that polymers cannot cut across each other. This is in effect a soft-core repulsion term, and the softness arises because we are studying a homopolymer network at a mesoscale, where polymers may pass by each other, without actually cutting across each other. The nonlocal attractive term gives rise to entanglement, as it causes portions of the network within the screening distance $1/\delta$ to be attracted to each other. Equation 4 is the basic statement of our theory. Note that the two terms we just discussed have signs opposite those of corresponding terms in theories of self-assembly¹⁰. The non-local attractive term invokes the notion that entanglement of polymers must lead to knotty configurations¹⁹. This attractive term can be seen intuitively to lead to the notion of trapping, and as such is slightly similar to treatments of entanglement in the literature which use Arrhenius-like rate theories to provide for escape of polymers from local entangled arrangements.

In what follows, we shall set $\gamma = \alpha^4$, and $\delta^2 = \sqrt{2}\alpha$, with $\alpha^2 = g^2/2$. A strong motivation for this choice of parameters is provided in Appendix A, where we use notions from gauge theory to derive Eqn.4, with the parameters having the forms given above. Another explanation for such a choice is as follows. With our choices for the parameters, U_{eff} in momentum space may be written as:

$$U_{\text{eff}} = \int \frac{d^3 k}{(2\pi)^3} \hat{c}^*(k) [-\sqrt{2}\alpha k^2 - \sqrt{2}\alpha k^2/(1 + \sqrt{2}k^2/\alpha)] \hat{c}(k) \quad (5)$$

where the carats indicate a Fourier transform. Thus we see that the choices made for the parameters are equivalent to generalizing the diffusion constant $g \equiv \sqrt{2}\alpha \rightarrow \sqrt{2}\alpha[1 + 1/(1 + \sqrt{2}k^2/\alpha)]$, i.e., a non-local diffusion constant is obtained. If we now extremize the functional, the Euler-Lagrange equations can be written in conservative form as:

$$\vec{\nabla} \cdot \vec{I}(\vec{s}) = 0$$

$$\vec{I}(\vec{s}) = \vec{\nabla} \int \frac{d^3 k}{(2\pi)^3} \exp(i\vec{k} \cdot \vec{s}) [1 + 1/(1 + \sqrt{2}k^2/\alpha)] \hat{c}(k) \quad (6)$$

where $\vec{I}(\vec{s})$ can be interpreted in the conventional manner as a mass current. The divergence-free nature of this current makes it clear that with our choice of parameters, our internal energy functional preserves number conservation. This is quite appropriate, since the

internal energy is the quantity which is conserved for isolated systems. For an arbitrary choice of parameters, the Euler-Lagrange equations have the form: $\vec{\nabla} \cdot \vec{I}'(\vec{s}) = \text{Source/Sink Terms}$, indicating that number conservation can be a problem.

While our choice of parameters may appear to be overly restrictive, it turns out to be sufficiently rich to provide a description of the onset of entanglement in polymers. We will not explore more general sets of parameters in this paper.

Before we can compare our theory with experimental data, we need to consider the fact that our system is not really isolated, and may be in contact with an energy reservoir, perhaps as it is being acted on by mechanical forces in a stress experiment. For a system in contact with an energy reservoir, the quantity that is conserved is the Helmholtz free energy¹⁷ $A = U_{\text{eff}} - ST$, where S is the entropy of the system. The entropy of our system will be approximated in the conventional manner¹⁸:

$$-\frac{S}{k} = \int d^3s \, c(\mathbf{s}) \ln[c(\mathbf{s})] \quad (7)$$

Note that we have ignored a term in the above expression which is linear in the normalized concentration field. This term can be absorbed into the definition of the usual Lagrange multiplier constraint for number conservation. This additional constraint is necessary, over and above the considerations which led to Eqn.5, because we are now considering the Helmholtz free energy rather than just the internal energy. In the homogeneous mean field approximation, the chemical potential can be easily shown to be zero. We shall utilize this approximation to facilitate computations. This entropy term provides the free energy a single minimum. To further ease computations, we shall expand $c \ln(c)$ in a power series about the characteristic inverse volume $l^{-3}(=1)$ in our dimensionless units), retaining terms up to fourth order:

$$(1+c) \ln(1+c) \approx c + \frac{c^2}{2} - \frac{c^3}{6} + \frac{c^4}{12} \quad (8)$$

This expansion yields one minimum, just as the exact expression for the entropy. Consequently, we do not expect this system to display a phase transition, but rather a crossover from an un-entangled state to a state of entanglement. Finally, we note that in our present theory, entropy yields the crucial nonlinear terms which will describe the crossover to a state of entanglement, in contrast to our gauge theory of self-assembly¹⁰ where entropy did not play a dominant role.

We define the two-point Green's function as usual via $\mathcal{S}(\vec{x}, \vec{x}') = \text{Lim}_{J \rightarrow 0} (\delta^2 / \delta J(\vec{x}) \delta J(\vec{x}')) Q[J]$, where $Q[J] = \int \mathcal{D}c \theta(1+c) \exp[-\beta(U_{\text{eff}} - ST) - \int d^3s J(\vec{s}) c(\vec{s})]$, where $\theta(1+c)$ is a step function that indicates a restriction to physically acceptable values of the concentration. In practice, we shall be restricting our attention to small deviations of c from its average, so that the step function is implicitly accounted for during calculations. In the quadratic approximation, the structure factor is:

$$\hat{S}_0(k) = \frac{1}{1 + \alpha' k^2 + \alpha'^2 k^2 / (1 + 2k^2 / \alpha')} \quad (9)$$

where $\alpha' = \sqrt{2}\alpha$. Equation 9 displays a peak at the origin, as one might expect from the fact that entanglement creates blobs which are distributed at random within the system. The width of the peak indicates an inverse of the correlation length between the blobs. With this physical interpretation, $\sqrt{\alpha}$ is a measure of the distance between concentration fluctuations (i.e. between points of entanglement). The decay of $\hat{S}_0(k)$ is affected by the value of α . As α decreases, the structure factor looks more diffuse. Thus, a decrease in α signifies a shift to a state of higher entanglement, as the concentration of entanglement points increases.

Our results can be understood compactly in terms of the parameter α , or equivalently, g , which may be identified with the self-diffusion coefficient of a polymer. As dictated by the discussion in section IV later in the paper, where by comparison with data on various polymers, we find that $\alpha \approx a_0 + a_1 M_n + a_2 M_n^2$, M_n being the average molecular weight of the system. The constants in this expression are such that $\alpha(M_n)$ decreases as M_n increases, as discussed above. Let us now make some more definitions, viz., N is the average chain length, the average chain density is $\tilde{c} = \rho N_{\text{avogadro}} / (\mu_0 N)$, N_e is the average chain length between consecutive points of entanglement, the entangled chain number density $c_e = \rho N_{\text{avogadro}} / (\mu_0 N_e)$, and the monomer number density $c_0 = \rho N_{\text{avogadro}} / \mu_0$, with ρ being the mass density of polymer, N_{avogadro} the Avogadro's number, and μ_0 the molecular weight of the monomer. l is the length scale in our theory and we shall take it to be $l = \lambda \tilde{c}^{-1/3}$, where λ is a parameter taken to be $(2/3)^{1/3}$ as it leads to an expression for the tensile modulus in the Gaussian approximation which agrees with the standard Wall theory result in the limit of short (entangled) states. We shall use the length l to scale all other lengths in the system. These ideas are slightly similar to Stillinger's in another context^{20,21}. By choosing our length scale in this fashion, it allows us to see how higher order corrections beyond the Gaussian approximation lead to an enhanced elastic modulus. In this manner we have attempted to relate our theory in an intimate fashion to the notion of entanglement.

III. BEYOND THE GAUSSIAN APPROXIMATION.

We shall now use diagrammatic methods to go beyond the Gaussian approximation to the structure function described at the end of the previous section. The reason is to be able to describe the crossover to a state of entanglement. As discussed in the previous section, the onset

of entanglement is not a phase transition, but simply a crossover.

Figures 1a and 1b show the basic vertices in our theory. The figure captions describe the Feynman rules which go with these vertices. We shall compute only the first non-vanishing terms which arise from each of these vertices. The first order contribution of the cubic term is zero, as follows from symmetry considerations. We have to go to the second order in the cubic term to obtain a *tadpole* diagram which is non-vanishing, as shown in Figure 2a. It serves to renormalize the correlation function in the long wavelength limit. Figure 2b is the other *setting sun* diagram which comes from the second order contribution of the cubic term. It may be expanded in powers of its argument k . The term proportional to k^2 helps to renormalize the *diffusion* constant g , and serves to diminish it, as one would expect entanglement to. Figure 3 shows the conventional *bubble* diagram coming from first order perturbation theory with the quartic term. It serves to renormalize the correlation function in the long wavelength limit.

In order to render the integrals in our theory finite in three dimensions, we shall use the following regularization scheme. We shall perform an expansion of the denominator of the Gaussian structure factor in powers of k . We shall retain terms up to $\mathcal{O}(k^6)$. This is essentially an expansion in inverse powers of α . This expansion yields the requisite higher order terms in the denominators of the Green's function to render our integrals finite, while ensuring that $\hat{S}_0(k) > 0$. This method has the advantage of retaining the correct long-wavelength behavior, at the expense of high momentum behavior. This is acceptable, since we do not expect our theory to be correct at small wavelengths in any event. We shall shortly compare our method with the conventional method of renormalization via counter-terms. Our single-particle Green's function in the Gaussian approximation is now taken to be:

$$\hat{S}_0(k) = \frac{1}{1 + 2\alpha'k^2 - 2k^4 + k^6/(2\alpha')} \quad (10)$$

With this definition, the net contribution from diagrams shown in Figures 2a and 3 is:

$$\Sigma_{2a+3}(\alpha) = -\left(\frac{3}{4}\right) \mathcal{S}_0(0) \quad (11)$$

Figure 2b yields a k -dependent contribution to the self energy:

$$\begin{aligned} \Sigma_{2b}(\vec{k}) &= \left(\frac{1}{4}\right) \int \frac{d^3k'}{(2\pi)^3} \hat{S}_0(k') \hat{S}_0(|\vec{k}' - \vec{k}|) \\ &\approx \delta a + \delta g k^2 + \mathcal{O}(k^4) \end{aligned} \quad (12)$$

where:

$$\begin{aligned} \delta a(\alpha) &\approx \frac{1}{128 \cdot 2^{1/4} \pi \alpha^{3/2}} \\ \delta g(\alpha) &\approx \left(\frac{1}{256 \pi \alpha^{1/2}}\right) \left(\frac{5}{2^{3/4} \alpha^2} - \sqrt{2}\right) \end{aligned} \quad (13)$$

where the integrals were performed by approximating the denominator of the Gaussian Green's function by terms up to $\mathcal{O}(k^2)$, as this suffices to guarantee convergence of the integrals, so that there is no sensitivity to the higher order terms neglected. We find that the contribution from Eqn.11 is extremely small compared to δa from Eqn.12. This is basically what happens in the usual renormalization scheme, where one eliminates terms such as $\mathcal{S}_0(0)$ (when Eqn.9 is used to perform the calculations) using appropriate counter-terms in the energy functional. In fact, in this scheme, $\hat{S}_0(k)$ decays quadratically with k , and the considerations used to obtain Eqn.13 automatically obtain.

With these expressions, we see that the renormalized value $g_R = g - \delta g$ of the diffusion constant decreases as α is decreased. As discussed in section II, the non-local attractive term in our free energy was identified with the formation of knotty configurations, or clusters¹⁹. We will therefore identify g_R with the dynamics of such clusters. Cluster dynamics have been recently observed using state-of-the-art techniques by Stepanek et al¹⁹. g_R is zero near $\alpha = 0.18$. Note that α decreases as we increase N the average chain length. We thus see that as entanglement increases, the effective diffusion constant decreases, analogous to *critical* slowing down. We are not aware of explicit experimental observations regarding the dynamics of clusters, with which g_R has been identified, near the cross-over threshold. This effect is similar to the considerations of Kavallis and Noolandi¹², Kroy and Frey¹³, and Broderix et al,²² who study the vulcanization transition in the mean field approximation, and find the diffusion constant going to zero as the vulcanization transition is approached. They point out that this result agrees with experimental results. Given the analogy between vulcanization (chemical cross-linking) and physical entanglement, we believe this result should be experimentally observable in entangled systems as well. Broderix et al obtained $g_R \rightarrow 0$ linearly with the average concentration. We have obtained a more complicated dependence on the concentration. We find that $\alpha \approx 0.18$ when the renormalized diffusion constant goes to zero. One could estimate α using results from the next section on the tensile modulus of polymers and experimental values for polymeric elastic moduli, and then obtaining a value for the critical N^* at which the effective diffusion constant goes to zero.

The origin of $\delta g > 0$ can be traced back to the nonlocal attractive term in U_{eff} , defined in Eqn.4. This nonlocal attractive term, which we interpreted as giving rise to entanglement, is responsible for a physical signature of the onset of entanglement, with $g_R \rightarrow 0$.

IV. TENSILE MODULUS.

It is well-known that the Wall theory result for the tensile modulus, while yielding the correct trend, does not agree with experimental data on moduli by a large factor. Edwards' application of deGennes's reptation model³ provides an enhancement factor over Kuhn's result, and shows conceptually how entanglement leads to an increase in the stiffness of the homopolymer system. We will show in this section how to obtain a similar result in our continuum treatment. More importantly, we will show we can go further, and describe a crossover, as the mean chain length between entanglements is decreased, to a regime where the tensile modulus, instead of remaining fairly constant, begins to increase extremely rapidly as a function of decreasing N_e . The reptation model is unable to accomplish this,⁴ as it assumes that the system is already in the entangled state, and does not account for inter-chain interactions, beyond assuming a preformed tube.

The Helmholtz free energy in the Gaussian approximation is given by:^{23,24}

$$\mathcal{F}_G = -\frac{3}{2}kTV\tilde{c}\hat{\mathcal{S}}_0(k=0) = -\frac{3}{2}kTV\tilde{c} \int d^3x \mathcal{S}_0(x) \quad (14)$$

We may represent a strained state of the system by the transformation $\vec{x} \rightarrow \vec{x}' = \vec{x} + \vec{u}(\vec{x})$ in the above equation. This is possible because $\mathcal{S}(\vec{x})$ in the above equation represents the density-density correlation function $\langle c(\vec{r})c(\vec{r} - \vec{x}) \rangle$, so that when the system is strained, $c(\vec{r} - \vec{x})$ in our theory shifts to $c(\vec{r}' - \vec{x}')$, where $\vec{r}' = \vec{r} + \vec{u}(\vec{r})$. For the case of homogeneous deformation, we shall take $\vec{u}(\vec{x}) = \vec{\epsilon} \cdot \vec{x}$, where ϵ is the strain tensor. The strain is assumed to be volume-preserving, so that $d^3x = d^3x'$. Our approach is similar to that of Castillo and Goldbart¹⁴. It is now easy to show, using a Taylor series expansion that the change in the pressure $P = -(\partial\mathcal{F}/\partial V)_{T,N}$ is:

$$\begin{aligned} \Delta P_G &\approx \frac{3}{2}kT\tilde{c}\hat{\mathcal{S}}_0(k=0)\epsilon_{\alpha\beta}\epsilon_{\gamma\delta}\mathcal{D}_{\alpha\beta\gamma\delta} + \mathcal{O}(\epsilon^4) \\ \mathcal{D}_{\alpha\beta\gamma\delta} &= (\delta_{\alpha\beta}\delta_{\gamma\delta} + \delta_{\alpha\gamma}\delta_{\beta\delta}) \end{aligned} \quad (15)$$

where the subscript G denotes the Gaussian approximation. As needed, we can consider the expansion of Free energy to include higher orders of the strain tensor²⁵. ΔP_G is a measure of the change per unit volume of the energy of the system under strain. In analogy with a simple harmonic oscillator, the force tensor which constrains the system from undergoing a strain $\vec{\epsilon}$ is given by $-3kT\tilde{c}\hat{\mathcal{S}}_0(k=0)\vec{\epsilon} : \vec{\vec{D}}$. Thus, the stress $\vec{\sigma}$ required to produce this strain is:

$$\vec{\sigma} = 3kT\tilde{c}\hat{\mathcal{S}}_0(k=0)\vec{\epsilon} : \vec{\vec{D}} \quad (16)$$

One may now readily write down the tensile modulus as:

$$Y_G = 3kT\tilde{c} \quad (17)$$

This is identical to the well-known Wall theory result obtained by in the limit of short (unentangled) chains. And it's origin is purely entropic. Our goal is to go beyond this result, and to do that, we shall *dress* the bare propagator $\hat{\mathcal{S}}_0(k)$ using the diagrams shown in Figures 2 and 3. This immediately leads to the renormalized result Y_R :

$$\begin{aligned} Y_R(\alpha) &= 3kT\tilde{c}\hat{\mathcal{S}}_R(k=0) \\ &= 3kT\tilde{c} \left[\frac{1}{1 - \Sigma_{2a+3}(\alpha) - \delta a(\alpha)} \right] \end{aligned} \quad (18)$$

The first of these equations is similar to the connection made between the structure factor in the long wavelength limit and the bulk modulus by Kirkwood²⁶.

The result of plotting the *entanglement* factor $\mathcal{Z} = Y_R/Y_G - 1$ as a function of $\alpha(N)$ is presented in Figure 4. We see that the enhancement factor, which is fairly constant above $\alpha = 0.2008$, begins to increase dramatically below this value of $\alpha = 0.2008$. As discussed in section II, decreasing α is equivalent to increasing N , the average number of links in a polymer. And increasing N is associated with increasing entanglement.

To see better the connection between our approach and the underlying chain parameters, we identify the prefactor $(\mathcal{Z}(\alpha) + 1)$ multiplying the Wall theory result with the enhancement obtained within the reptation model⁴, i.e., $\mathcal{Z}(\alpha) + 1 \equiv (Nb^2/a^2)$, where b is the monomer length, and a is the diameter of the tube in the reptation model. This identification gives us a relation between α and the parameters of reptation theory. It also gives us a relation between our theory and the underlying chain parameters such as N , the average number of links, and N_e , the average number of links between successive points of entanglement, viz., $N_e^{-1} = (b^2/a^2)$. In fact, we can provide such an analytic, approximate relation in the following manner. Based on numerical estimates of $\mathcal{S}_0(0)$, we find that in the the highly entangled state, $|\delta a(\alpha)| \gg |\Sigma_{2a+3}(\alpha)|$. Then, using Eqn.13, we immediately obtain:

$$\begin{aligned} \alpha(N_e, N) &\approx \kappa(1 - N_e/N)^{-2/3} \\ \kappa &= \left(\frac{1}{128 \cdot 2^{1/4} \pi} \right)^{2/3} \end{aligned} \quad (19)$$

It should be noted that this particular scaling relation Eqn.19 holds only in the limit of highly entangled states. While we have denoted the explicit dependence on N_e and N separately, it should be noted that N_e itself depends on the chain length N . More generally, the advantage of our theory is that the enhancement factor $[\mathcal{Z}(\alpha(N)) + 1]$ can change continuously from a value of unity in the unentangled state, to a fairly large number as the system becomes increasingly entangled. As discussed earlier, the reptation model on the other hand

presupposes the formation of tube-constraint caused by polymer chains surrounding any given chain. As such it applies only in the highly entangled state.

We introduced our theory in section II in a phenomenological fashion, and so the best way to establish the validity of our theory is to compare the results of our theory with experiment, the connection with the underlying chain parameters (Eqn.19) notwithstanding. However, we are not aware of experimental data on the elastic properties of entangled polymers detailing in a precise manner the cross-over to the entangled state.

Nevertheless, we were able to find an experimental paper by Onogi et al²⁷ which provides systematic viscoelastic data on amorphous polystyrene in the melt state, over a wide range of frequencies and molecular weights (and having a low degree of polydispersity). We were able to obtain static shear moduli from the plateau moduli given in this paper. The conventional assumption of incompressibility then says that Young's modulus is three times the shear modulus. Armed with these data, we were able to obtain a parameterization of α as function of the molecular weight $M_n (= \mu_0 N)$ (see Table 1 and Figure 5). This parameterization is consistent with the stress-strain data provided by Bicerano et al⁸. This parameterization is also consistent with Eqn.19. Equation 19 implies that for very large molecular weights, $\alpha \rightarrow \kappa \approx 0.01635$. From Figure 5, we see such values for α occurring at the high end of the range of molecular weights. The parameterization depicted in Figure 5 may be thought of as a power series expansion of Eqn. 19.

The cross-over between the un-entangled state and entangled state appears to take place between $M_n \approx 113,000$ and $M_n \approx 60,000$, as the plateau in the storage moduli measurements disappears somewhere between these two values of the molecular weights²⁷. Unfortunately, this cross-over is not described well by these data, as measurements in the cross-over region are unavailable. This could well be due to the critical slowing down which our theory predicts will occur during the cross-over (see section III). As can be seen from Table 1 and Figure 5, the data develops noise at the low end of the range of molecular weights. And this is consistent with the prediction of critical slowing down, as the system takes very long to settle into a metastable state. Since we have a cross-over phenomenon, it is difficult to pinpoint a single value of M_n at which the transition to the entangled state occurs. But based on Figure 6, in which the logarithm of the enhancement factor has been plotted as a function of M_n , we see that it starts to become appreciable ($\gg 1$) in the neighborhood of $M_n \sim 50,000$. The theory thus predicts that it is in this neighborhood that the cross-over takes place. It would be very interesting to see more experiments performed in the future, say for amorphous polystyrene, with M_n in the range just discussed, to see if the path of the cross-over agrees with that shown in Figure 6. It is even more important to do such experiments to ascertain if the critical slowing down predicted in section III does indeed occur.

V. CONCLUSIONS

We postulated an extension of the Cahn-Hilliard functional to describe entanglement in polymers. We extended the Cahn-Hilliard functional with two terms. One is an attractive nonlocal term which describes the effect of entanglement, and the other a local repulsive term indicative of excluded volume interactions. We showed in Appendix A how this extended functional can be derived using notions from gauge theory. Using field theoretic techniques to go beyond the Gaussian approximation, we showed that the onset of entanglement is a crossover phenomenon, signaled by the effective diffusion constant going to zero. We developed a simple model to connect the single parameter in our theory with the parameters of the underlying chains by comparison with available experimental data on amorphous polystyrene melts. A reasonable estimate for the critical partial chain concentration at which this crossover occurs was obtained. While this is consistent with available data, further experiments to determine the details of this cross-over were suggested, especially to ascertain if the critical slowing down predicted in this paper does indeed occur.

VI. ACKNOWLEDGMENTS

I would like to acknowledge discussions with Brian Kendrick regarding the gauge theoretic formulation of the problem. I would also like to thank Dr. J. Bicerano for kindly supplying raw experimental stress-strain data⁸ on amorphous polystyrene utilized for a consistency check of the theory developed in this paper. The work described in this paper was done under aegis of the LDRD-CD program on polymer aging at the Los Alamos National Laboratory.

APPENDIX A.

In this appendix, we shall show how to derive Eqn.4, along with the choice of parameters made in section II, using notions from gauge theory. Let us start with:

$$\beta u_0(c(\mathbf{s})) = \left(\frac{g}{2}\right) \frac{\partial c(\mathbf{s})}{\partial s_i} \frac{\partial c(\mathbf{s})}{\partial s_i} \quad (\text{A.1})$$

where the variables have been defined in section II. We will use this form as our starting point to generate a more complete energy functional using gauge invariance.

From Eqn.A.1 we see that u_0 is invariant under global translations of $c(\vec{s})$, i.e. under $c(\vec{s}) \rightarrow c(\vec{s}) + h$ where h is a constant. And the appropriate group to consider is T_1 . The physical origin of this group can be traced back to the fact that the quadratic (positive, semi-definite) form

of the energy density is dictated by expanding the internal energy around a minimum, in a Landau-like fashion. Physicality of T_1 transformations demands that $c' + c_e > 0$, where c' denotes the deviation of the specie concentration from its average, and that number conservation is guaranteed. These physical constraints will be incorporated into the evaluation of the partition function, *after* gauging U_0 , in a manner similar to applying gauge constraints in QFT.

Our physical motivation for seeking local gauge invariance under T_1 is the same as that of Yang and Mills²⁹, and in quantum electrodynamics (QED), where one observes the invariance of the noninteracting Lagrangian under certain global transformations. One then demands covariance of the theory when these symmetry operations are *local* i.e., when the transformations are space-time dependent. A reason for this, as given by Yang and Mills, is that one can now freely interchange between the fields as one moves through space and time, while leaving the physics covariant. It is important to note that gauge theory in QFT is *not* a result of the fact that the phase of the field is not measurable. In fact, Aharonov and Bohm showed many years ago that the phase in quantum mechanics is indeed observable. Local transformations under T_1 generate concentration fluctuations which arise from entanglement.

Following Yang and Mills,²⁹ local gauge invariance of u_0 under T_1 motivates us to define new fields \mathbf{b} , which have invariance properties appropriate to T_1 . We define a covariant derivative $\frac{\partial}{\partial s_i} \rightarrow (\frac{\partial}{\partial s_i} + q\tau b_i)$, where $\tau = \frac{\partial}{\partial c}$ is the generator of T_1 , q is a ‘charge’, or equivalently, a coupling constant, and the b -fields are analogs of the magnetic vector potential in electrodynamics. In our previous theory of self-assembly¹⁰, gauge fields arose from the underlying covalent bonds between the two species in the system. In the present case, where we wish to describe entanglement, the gauge fields are to be thought of as arising purely from statistical considerations alone. On the other hand, chemical cross-linking would provide a physical origin for the b -fields in vulcanized systems. The energy functional for the b -fields is defined à la Yang and Mills, via the minimal prescription. With this, our original internal energy density is transformed into:

$$\beta u_0 \rightarrow \beta u = \beta u_0 + \beta u_{int} + \beta u_{YM} \quad (\text{A.2})$$

where u_{int} refers to the interaction energy density, and u_{YM} is the energy density associated with the Yang-Mills b -fields alone. Equivalently, we may define the total energy functionals associated with these energy densities:

$$\beta U_0 \rightarrow \beta U = \beta U_0 + \beta U_{int} + \beta U_{YM},$$

where

$$\beta u_{int} = \vec{J}(c) \cdot \vec{b}(\mathbf{s}) + f \vec{b}(\mathbf{s}) \cdot \vec{b}(\mathbf{s}) \quad (\text{A.3})$$

with

$$\vec{J}(c) = gq\vec{\nabla}c \quad (\text{A.4})$$

$$f = \left(\frac{gq^2}{2} \right) \quad (\text{A.5})$$

We need one more definition for completeness:

$$\beta u_{YM} = \left(\frac{1}{4} \right) \left(\frac{\partial b_i}{\partial s_j} - \frac{\partial b_j}{\partial s_i} \right) \left(\frac{\partial b_i}{\partial s_j} - \frac{\partial b_j}{\partial s_i} \right) \equiv \frac{\vec{B}^2}{4} \quad (\text{A.6})$$

This equation can be cast into the following form:

$$\beta u_{YM} = - \left(\frac{1}{2} \right) b_i \nabla^2 b_i \quad (\text{A.7})$$

Eqn.A.7 is obtained via an integration by parts, in the transverse gauge. Since we are dealing with an Abelian gauge theory, it is permissible to insert this transverse gauge manually, without resorting to the formal machinery of Faddeev and Popov.

Again using the transverse gauge and integrating by parts, it is clear that:

$$\begin{aligned} \int d^3s \vec{\nabla}c(\vec{s}) \cdot \vec{b}(\vec{s}) &= - \int d^3s c(\vec{s}) [\vec{\nabla} \cdot \vec{b}(\vec{s})] \equiv 0 \\ &= i \int d^3s \vec{\nabla}c(\vec{s}) \cdot \vec{b}(\vec{s}) \end{aligned} \quad (\text{A.8})$$

It is this crucial identity which allows us to get the precise form for Eqn.4, which we motivated in section II using an intuitive approach. It is the nature of the T_1 group which permits this manipulation to go through successfully. In our earlier paper¹⁰, where we used the $SO(2)$ group, such a manipulation would not have availed us any advantage.

Note that we are utilizing a non-relativistic version of the Yang-Mills procedure, since we are only concerned with time-independent problems. Furthermore, since we are concerned with translations in T_1 , there is only a single generator to contend with, so that the resulting functional is only quadratic and not quartic in the b -fields.

It is important to emphasize that the usual application of the Yang-Mills procedure in QFT implies the existence of fundamental interactions. In our case, we are applying the principle of local gauge invariance at the *mesoscale*. Consequently, we do not expect to discover any new fundamental interactions by using gauge invariance. Rather, we interpret the new b -fields as yielding correlations between the concentration fields. These correlations could also be thought of as effective interactions, which arise at the mesoscale from the underlying electrostatic interactions between molecules.

The partition function we need to evaluate is now:

$$Q' = \int \mathcal{D}c \theta(c) \prod_{k=1,3} \mathcal{D}b_k \exp - \beta(U_0 + U_{int} + U_{YM}) \quad (\text{A.9})$$

Equation A.9 is a functional integral, where the step functions denoted by θ imply that we must restrict integration to positive semi-definite values of the fields.

Since the b -fields appear only quadratically in the above functional, it is straightforward to integrate over them, and obtain an effective internal energy functional involving only c , upon using Eqn.A.8. The result is:

$$\begin{aligned}\beta U_{\text{eff}} &= \beta U_0 + \beta \Delta U_{\text{eff}} \\ &= \beta U_0 + \frac{1}{4} \int d^3 s \int d^3 s' J_i(c(\mathbf{s})) \left(\frac{1}{f - \frac{1}{2} \nabla^2} \right)_{\mathbf{s}, \mathbf{s}'} J_i(c(\mathbf{s}'))\end{aligned}\quad (\text{A.10})$$

Note that in doing so, we have ignored an overall trivial normalization constant that appears in the evaluation of the partition function Q' . This is permissible, as this factor cancels during the evaluation of averages of observable quantities.

To reveal the physics in this effective functional, we perform some straightforward algebra to write our result as:

$$\begin{aligned}\beta U_{\text{eff}} &= \beta U_0 + \left(\frac{\alpha^2}{2} \right) \int d^3 s \, c(\mathbf{s}) c(\mathbf{s}) \\ &- \left(\frac{\alpha^4}{2\pi} \right) \int d^3 s \int d^3 s' \, c(\mathbf{s}) \frac{\exp(-\sqrt{2\alpha^2/g} |\mathbf{s} - \mathbf{s}'|)}{|\mathbf{s} - \mathbf{s}'|} c(\mathbf{s}')\end{aligned}\quad (\text{A.11})$$

where $\alpha^2 = g^2 q^2 / 2$ (we shall use units in which $q=1$). Note that U_{eff} is quadratic, the generator of T_1 making sure that higher order terms do not appear in our functional. Equation A.11 is one of the main results of our paper, and provides a deeper motivation for the model developed in section II on intuitive grounds. As discussed in section II, the form of Equation A.11 guarantees number conservation. Equation A.11 shows that entanglement may be understood in the context of a mesoscopic gauge theory. Note that the two terms we just discussed have signs opposite those of corresponding terms in theories of self-assembly¹⁰. We thus see that using T_1 instead of $SO(2)$ in the previous theory¹⁰ has led to a qualitatively different theory. Finally, this approach provides an alternative gauge theory of polymer entanglement than the one given by Brereton³⁰. In this paper, Brereton works explicitly with entangled strands of polymers and provides a static theory which yields e.g. a renormalized expression for the radius of gyration. It would be interesting to see how Brereton's theory could be generalized to include dynamics as well.

- ³ M. Doi, *Introduction to Polymer Physics*, Oxford University Press, Oxford (1996).
- ⁴ M. Doi, S.F. Edwards, *The Theory of Polymer Dynamics*, Oxford University Press, Oxford (1986).
- ⁵ S. Prager, H.L. Frisch, J. Chem. Phys., **46**, 1475 (1966).
- ⁶ K. Koniaris, M. Muthukumar, J. Chem. Phys., **103**, 7136 (1995).
- ⁷ Y. Termonia, P. Smith, Macromolecules, **20**, 835 (1987); Y. Termonia, Macromolecules, **29**, 4891 (1996).
- ⁸ J. Bicerano, N.K. Grant, J.T. Seitz, K. Pant, to appear in Macromolecules (1997).
- ⁹ T. Holtz, H.L. Trautenberg, D. Goritz, Phys. Rev. Lett., **79**, 2299 (1997).
- ¹⁰ S.M. Chitanvis, Phys. Rev. E **57**, 1921 (1998); also available in post script format at <http://www.t12.lanl.gov/~shirish/preprints.html>.
- ¹¹ J.W. Cahn and J.E. Hilliard, J. Chem. Phys., **28**, 258, (1958).
- ¹² T.A. Kavallis and J. Noolandi, Phys. Rev. Lett., **59**, 2674 (1987).
- ¹³ K. Kroy and E. Frey, Phys. Rev. Lett., **77**, 306 (1996).
- ¹⁴ H.E. Castillo and P.M. Goldbart, preprint, cond-mat/9712050.
- ¹⁵ R.T. Deam and S.F. Edwards, Phil. Trans. R. Soc., **280A**, 317 (1976).
- ¹⁶ P.G. deGennes, *Scaling concepts in polymer physics*, (Cornell University Press, Ithaca, N.Y. 1979).
- ¹⁷ H.B. Callen, *Thermodynamics*, p. 106, J. Wiley & Sons, Inc., N.Y. (1960).
- ¹⁸ H.J. Raveché, J. Chem. Phys. **55** 2242, (1971).
- ¹⁹ P. Stepanek and Wyn Brown, Macromolecules **31**, 1889 (1998).
- ²⁰ F.H. Stillinger, J. Chem. Phys., **78**, 4654 (1983).
- ²¹ C. Carraro, Physica A, **236**, 130 (1997).
- ²² K. Borderix, P.M. Goldbart, A. Zippelius, Phys. Rev. Lett., **79**, 3688 (1997).
- ²³ P. Ramond, *Field Theory: A Modern Primer*, page 126, The Benjamin/Cummings Pub. Co., (1981).
- ²⁴ J.J. Binney, N.J. Dowrick, A.J. Fisher, M.E.J. Newman, *The theory of critical phenomena: An introduction to the renormalization group*, Oxford Science publications, Oxford (1995).
- ²⁵ N. Triantafyllidis and S. Bardenhagen, Journal of Mech. and Phys. of solids, **44**, 1891 (1996).
- ²⁶ J.G. Kirkwood, R.J. Goldberg, J. Chem. Phys., **18**, 54 (1950).
- ²⁷ S. Onogi, T. Masuda and K. Kitagawa, Macromolecules **3**, 109 (1970).
- ²⁸ W.M. Graessley, *The entanglement concept in Polymer Rheology*, Adv. Poly. Sci. **16**, Springer-Verlag, Berlin (1974).
- ²⁹ C.N. Yang and R.L. Mills, Phys. Rev., **96**, 191 (1954).
- ³⁰ M.G. Brereton, J. Molec. Struct. **336**, 191 (1995).

¹ C.G. Moore and W.F. Watson, J. Polymer Sci., **19**, 237 (1956).

² P.J. Flory, N. Rabjohn, M.C. Shaffer, P. Polymer Sci., **4**, 225 (1949).

TABLE I. Fitted values of α obtained in comparison with experimental data from Onogi et al on amorphous polystyrene melts at 160 °C. Young's modulus is denoted by Y .

Molecular weight	Y_{exptl} (psi)	α (fitted)
581,000	93	0.0166
513,000	84	0.0167
351,000	66	0.0171
275,000	65	0.0173
215,000	62	0.0177
167,000	56	0.0184
113,000	106	0.0179

FIG. 1. (a) is a pictorial representation of the cubic term in A . Each leg corresponds to a factor of c , the field. The intersection of the three legs symbolizes a factor of $\gamma = 1/6$, the coupling constant. (b) is a pictorial representation of the quartic term in A . A factor of $-1/12$ is to be inserted at the intersection.

FIG. 2. (a) represents the *tadpole* diagram which is crucial in our calculations. (b) represents the *setting sun* diagram. Both (a) and (b) are second order contributions to the correlation function coming from the cubic interaction term, the first order corrections being null.

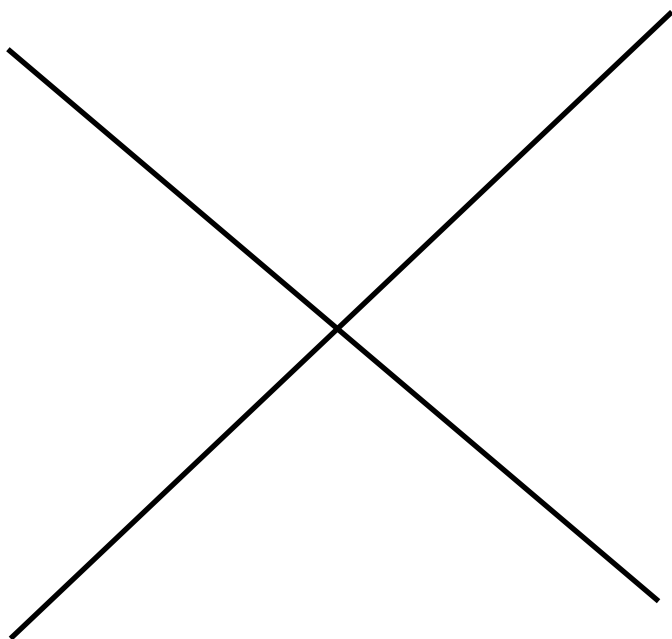
FIG. 3. This figure represents 1-loop (bubble) contribution from the quartic interaction term in A .

FIG. 4. This is a plot of $\mathcal{Z} = Y_R/Y_G - 1$ as a function of α . Notice that the factor is virtually constant above $\alpha = 0.20$, followed by a dramatic increase below this value of α . Approximations employed in the calculation cause the entanglement factor to diverge at $\alpha \approx 0.01$. Remember, decreasing α corresponds to increasing entanglement.

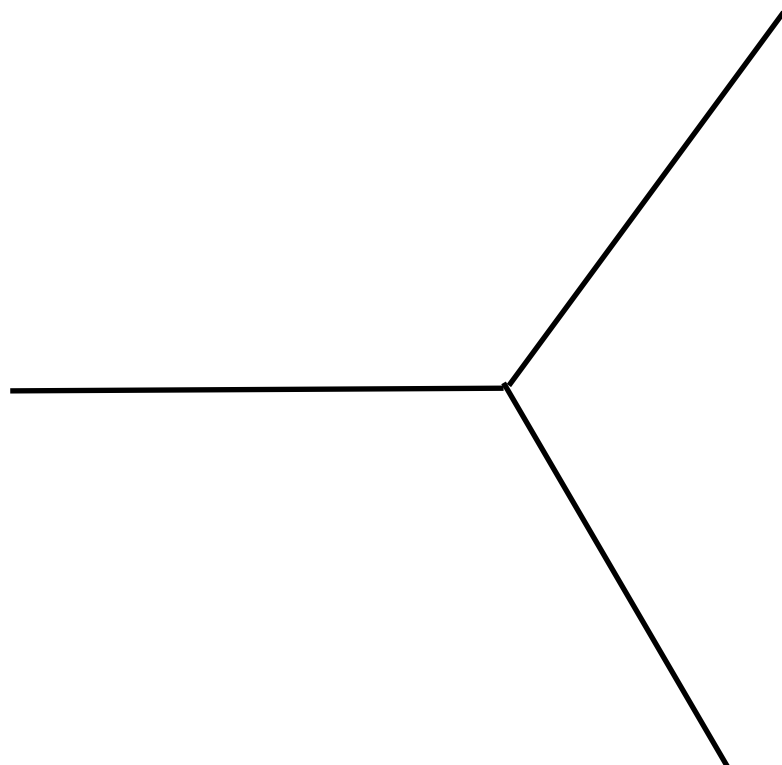
FIG. 5. This dots are the values of α required to achieve agreement with experimental values of moduli of amorphous polystyrene melts for a range of M_n . The solid line indicates a least squares fit obtained using $\alpha(M_n) = a_0 + a_1 M_n + a_2 M_n^2$, with $a_0 = 0.0189$, $a_1 = -6.18 \times 10^{-9}$, $a_2 = 3.89 \times 10^{-15}$. Caution should be exercised in using this expression to estimate α too far from the range in which the fit was made.

FIG. 6. Plot of $\text{Log}[\mathcal{Z}]$ as a function of the molecular weight M_n . Notice that \mathcal{Z} begins to attain nontrivial values above $M_n \sim 5 \times 10^4$. The curve indicates the path of the cross-over from an un-entangled state to an entangled state.

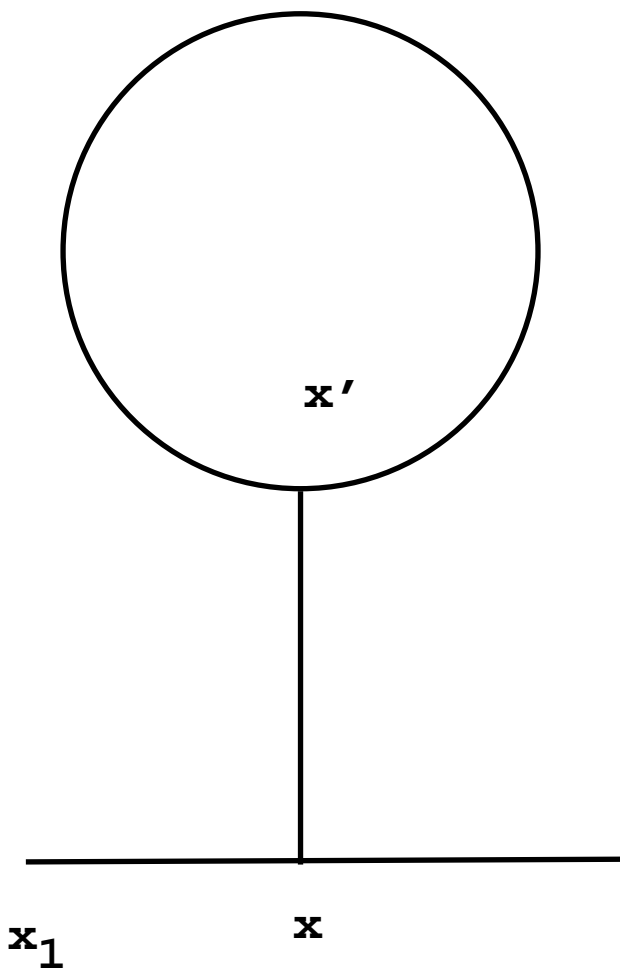
Chitanvis, Fig. 1



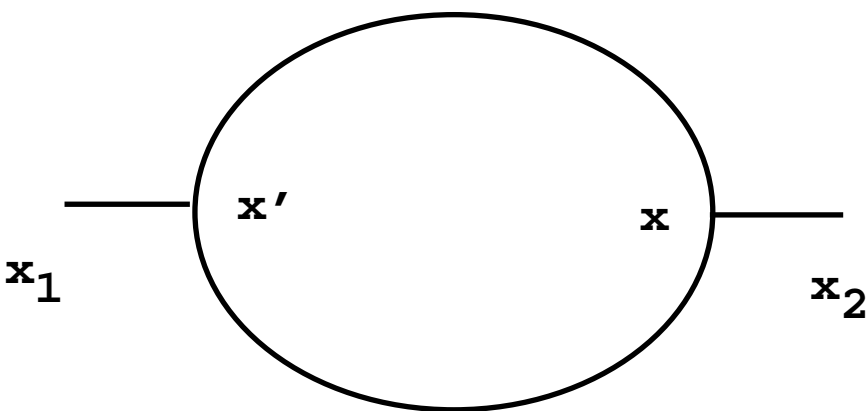
b



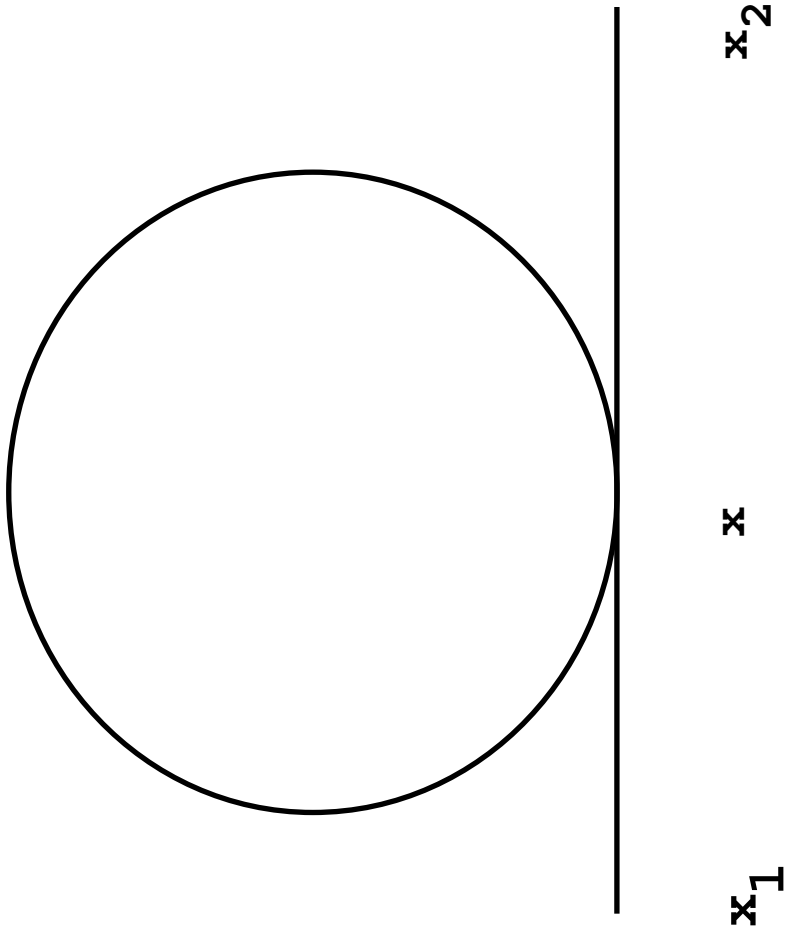
a



(a)



(b)



Chitanvis, Fig. 4

